Travelling with a parasite: the evolution of resistance and dispersal syndromes during experimental range expansion

Giacomo Zilio, Louise Nørgaard, Claire Gougat-Barbera, Matthew Hall, Emanuel Fronhofer, Oliver Kaltz

PROCEEDINGS OF
THE ROYAL SOCIETY B
BIOLOGICAL SCIENCES

Travelling with a parasite: the evolution of resistance and dispersal syndromes during experimental range expansion

Journal:	*Proceedings B*
Manuscript ID	RSPB-2022-0157
Article Type:	Research
Date Submitted by the Author:	26-Jan-2022
Complete List of Authors:	Zilio, Giacomo; University of Montpellier Nørgaard, Louise; Monash University Gougat-Barbera, Claire; University of Montpellier Hall, Matthew D.; Monash University, School of Biological Sciences Fronhofer, Emanuel; University of Montpellier Kaltz, Oliver; University of Montpellier
Subject:	Evolution < BIOLOGY, Ecology < BIOLOGY
Keywords:	Dispersal syndromes, eco-evolutionary dynamics, host-parasite interactions, invasion front, range expansion, resistance
Proceedings B category:	Evolution

Author-supplied statements

Relevant information will appear here if provided.

Ethics

Does your article include research that required ethical approval or permits?:
This article does not present research with ethical considerations

Statement (if applicable):
CUST_IF_YES_ETHICS :No data available.

Data

It is a condition of publication that data, code and materials supporting your paper are made publicly available. Does your paper present new data?:
Yes

Statement (if applicable):
The data from this study are available at https://doi.org/10.5281/zenodo.5907048

Conflict of interest

I/We declare we have no competing interests

Statement (if applicable):
CUST_STATE_CONFLICT :No data available.

Travelling with a parasite: the evolution of resistance and dispersal syndromes during experimental range expansion

Giacomo Zilio[1#*], Louise S. Nørgaard[2#], Claire Gougat-Barbera[1], Matthew D. Hall[2], Emanuel A. Fronhofer[1] & Oliver Kaltz[1*]

Giacomo Zilio[1#*], gcm.zilio@gmail.com, ORCID ID: https://orcid.org/0000-0002-4448-3118

Louise S. Nørgaard[2#], lnorga10@hotmail.com, ORCID ID: https://orcid.org/0000-0002-0938-0017

Claire Gougat-Barbera[1], claire.gougat-barbera@umontpellier.fr, ORCID ID: unavailable

Matthew D. Hall[2], matthew.hall@monash.edu, ORCID ID: 0000-0002-4738-203X

Emanuel A. Fronhofer[1], emanuel.fronhofer@umontpellier.fr, ORCID ID: https://orcid.org/0000-0002-2219-784X

Oliver Kaltz[1*], oliver.kaltz@umontpellier.fr, ORCID ID: https://orcid.org/0000-0002-7154-0456

[1] ISEM, University of Montpellier, CNRS, EPHE, IRD, Montpellier, France.

[2] School of Biological Sciences and Centre for Geometric Biology, Monash University, Melbourne, Australia

[#] Shared first-author contribution

* Corresponding author: gcm.zilio@gmail.com, oliver.kaltz@umontpellier.fr

Abstract

Rapid evolutionary changes during range expansions can lead to the divergence between range core and front populations, with the emergence of dispersal syndromes. Besides intraspecific effects, range expansions may be impacted by interspecific interactions such as parasitism. Yet, despite the potentially large impact of parasites imposing additional selective pressures on the host, their role on range expansions remains largely unexplored. Here, we investigated whether parasites affect the evolution of host dispersal syndromes during spatial spread. Using populations of the ciliate *Paramecium caudatum* and its bacterial parasite *Holospora undulata* spreading in microcosm landscapes, we studied experimental range expansions under the presence or absence of the parasite. We found that range expansion and parasite treatments acted independently on the evolution of host dispersal syndromes. Front host populations showed different trait associations between swimming behaviour and population growth parameters than core populations, indicating divergent evolution. The presence of parasites reshaped these trait associations and divergence between front and core, with hosts exposed to the parasite exhibiting overall reduced dispersal, but increased resistance. Our work shows that host-parasite interactions during range expansions can shift the contenders to novel evolutionary trajectories and may influence the speed of the range expansion itself and of spreading epidemics.

Keywords

Dispersal syndromes, eco-evolutionary dynamics, host-parasite interactions, invasion front, range expansion, resistance

Introduction

Species range expansions are increasing in frequency in response to rapidly changing environments [1] and becoming crucial to reducing the risk of extinction [2]. While ecological and evolutionary processes have been well explored for single species, we are still lacking a good community perspective of range shifts [3,4]. Species might rarely "travel alone", and it is conceivable that interactions with other organisms facilitate or slow down spatial spread, and add new selection pressures while a species is spreading.

Antagonistic species interactions have been suggested a major factor defining species ranges [5,6]. Parasitism, for example, are ubiquitous and exert strong demographic and evolutionary pressures on the host, which can limit geographic ranges as has been shown in some theoretical models [7–9]. In fact, parasites may re-enforce range limits by reducing dispersal and/or by imposing additional mortality in already small populations at the front. This might be the case in the cane toad [10,11] and in other natural systems [12–14]. Adaptation to parasite attack may remove such range limits, but potentially also affect the evolution of other traits known to be selected at range fronts. This could produce eco-evolutionary feedbacks that will not only influence rates of spatial spread of the host species, but also impact parasite propagation in the target species, or spill-over of disease to other species along the way [15,16]. Further, parasites can cause knock-on effects on interactions with other species in the community [17,18] and affect ecosystem functioning [19].

Concomitant with antagonistic species interactions, range expansions often involve stochastic genetic changes in small vanguard front populations (via drift or founder bias), but also targeted evolution of dispersal due to spatial selection, spatial assortative mating and kin competition [20,21]. Dispersal evolution likely entails concerted changes in life-history, behavioural or physiological traits, leading to so-called dispersal syndromes [22,23]. Thus, the underlying genetic architecture and covariation among these traits will be critical to responses to selection at range fronts. Indeed, it has been shown for various biological systems that dispersal is a heritable trait and that covariation with other traits has a genetic basis [24], making it possible for selection to drive the divergence between core and front populations [25,26]. This is illustrated by the introduced cane toad (*Rhinella marina*) in Australia, where the evolution of dispersal and other life-history traits promoted the speed of spread at the invasion front [27–29]. Similar results were found for the invasive ladybird *Harmonia axyridis* [30], and in laboratory range expansions using experimental evolution approaches [31–33].

We currently know relatively little about parasite-mediated selection at range fronts and its consequences for dispersal syndrome evolution [3,4]. While a considerable bulk of literature exists on resistance evolution in host-parasite metapopulations [34,35], there is no specific theory in the context of range expansion.

Intuitively, we may expect that virulent parasites select for increased resistance and that this removes a parasite-imposed range speed limit. Such a case of resistance evolution has been found for populations of the cane toad infested by lung-worms at the range margin [36]. Theory further suggests that natural enemies select for changes in host dispersal. For example, parasite-induced fluctuations in host population dynamics can modify environmental predictability and fitness expectations, and consequently favour increased host dispersal [37,38]. Parasites may also select for plastic responses in dispersal, with sometimes counter-intuitive consequences for the spread of infection [39].

However, few if any studies have considered the joint action of parasite-mediated selection and spatial selection, and hence the interplay between the evolution of resistance and dispersal-related traits. Selection for resistance can be rapid and strong, but also modify genetic correlations with other life-history traits [40,41], often involving trade-offs [42,43] that constrain evolutionary trajectories. Such constrains may also concern dispersal syndromes. Our hypothesis it that dispersal syndrome might be different in the presence of the parasite, especially if there are trade-offs between dispersal and resistance.

Using experimental evolution, we investigated the effect of a parasite on the emergence of dispersal syndromes. In a long-term experiment, we mimicked range expansions in interconnected microcosms of the freshwater protist *Paramecium caudatum* and its bacterial parasite *Holospora undulata*. In a range front treatment, the paramecia were constantly selected to disperse into a new microcosm, whereas in the range core treatment, only the non-dispersing fraction of the population was maintained. Range and core treatments were established for infected and uninfected populations. Evolved hosts were assayed for six traits, including dispersal, resistance, population growth characteristics and swimming behaviour. We found substantial divergence in multiple phenotypic trait space, attributable to the combined additive effect of our experimental treatments. A dispersal syndrome emerged, with higher dispersal, equilibrium density and movement tortuosity in the front treatment, and higher growth rate and swimming speed in the core treatment. Parasite-mediated selection affected these trait relationships. Namely, front populations evolving with the parasite were more resistant, but also dispersed less than their parasite-free counterparts. The parasite-driven evolution of such novel characteristics may influence the speed of range expansions, but also the risk of spreading epidemics, which can have important implications for biological control, conservation and management decisions.

Material and methods

Study system

Paramecium caudatum is a freshwater filter-feeding ciliate with a world-wide distribution [44]. Ciliates typically exhibit a nuclear dimorphism: The “germ-line” micronucleus is active during the sexual stage, while

the highly polyploid "somatic" macronucleus regulates gene expression during the asexual stage, when replication occurs through mitotic division. In this experiment, clonal populations were maintained asexually (max. 1-2 population doublings per day at constant 23°C) in 50 mL tubes, using a sterilised lettuce medium (1g dry weight of organic lettuce per 1.5l of Volvic™ mineral water), supplemented *ad libitum* with the bacterium *Serratia marcescens* as a food resource (referred to as "bacterised medium" or "medium", hereafter). The gram-negative bacterium *Holospora undulata* is an obligate parasite, infecting the micronucleus of *P. caudatum* [45]. The infection life cycle comprises both horizontal and vertical transmission. *Paramecium* ingest infectious forms from the aquatic environment, which subsequently colonise the micronucleus and differentiate into multiplying reproductive forms; these reproductive forms are vertically transmitted to the daughter cells of mitotically dividing hosts. The infection life cycle is completed when reproductive forms differentiate into infectious forms, which are then released during host cell division or upon host death. Infection reduces cell division and survival of the *Paramecium*, as well as dispersal [46–48]. Experimental evolution of resistance to this parasite was demonstrated in previous long-term experiments and can come at reproductive costs [49,50].

Experimental protocols

(i) Long-term range expansion experiment

Dispersal in two-patch systems

We used two-patch systems for this selection experiment (Supplementary Information, Fig. S1). The systems were built from two 14 mL plastic tubes ("core patch" and "front patch") interconnected by 5-cm silicon tubing (0.6 mm inner diameter) serving as a corridor through which the *Paramecium* can actively swim. We define dispersal as the active displacement of *P. caudatum* from the core patch to the front patch. In the long-term experiment, short episodes of dispersal (3h) alternated with periods of population growth and maintenance (1 week). For a dispersal episode, we filled the two-patch system with 9.5 mL of fresh bacterised medium and then blocked the corridor with a clamp. The core patch was filled with c. 8ml of culture containing *Paramecium* (≈ 2000 individuals), whereas the front patch was only topped up with non-bacterised medium and was thus "empty". After removal of the clamp, *Paramecium* could freely disperse to the front patch or to stay in the core. After three hours, we blocked the corridor and estimated the cell density in the core and front patch, by sampling up to 1mL from each tube and counting the number of individuals under a dissecting microscope. The dispersal rate is thus the number of dispersers divided by the total number of individuals in the two-patch systems, divided by 3 hours.

Range expansion treatments

Two selection treatments were imposed. In the range front treatment, only *Paramecium* that had dispersed into the front patch were maintained and allowed to grow for 1 week until the next episode of dispersal.

Conversely, in the core selection treatment, only the non-dispersing *Paramecium* were maintained and allowed to regrow. These contrasting selection protocols were continued for a total of 26 cycles. The front selection treatment mimics the leading front of range expansion or a biological invasion, with populations continuously dispersing into a new microcosm. Populations from the core selection treatment stay in place and continuously lose emigrants. Each new growth cycle was started by placing on average 200 paramecia from front and core selection treatments in 20 mL of fresh bacterised medium, and equilibrium density was then reached within the following 3-4 days. The experiment was conducted with a single host line [47]. This line (63D) had undergone three years of parasite-free core selection prior to the present experiment; initially started from a mix of strains, it has become fixed for a single haplotype [51].

Parasite treatment

Core and front treatments were established for both infected and uninfected populations. Starting from a 63D laboratory culture, infected and uninfected selection lines were established. The parasites were taken from an ongoing experiment [47] that had already been imposing core and front selection on infected 63D populations for about 8 months (30 cycles). Using standard protocols (see S2), we extracted infectious forms of the parasite from 5 core selection lines and from 5 front selection lines, which were then used to inoculate our new, naive 63D hosts. In other words, we continued core and front selection treatments for the parasite, but replaced the previous hosts by new unselected hosts. In addition to these 10 infected selection lines, we established 3 uninfected front-selection lines and 3 uninfected core-selection lines as controls for a total of 16 selection lines.

(ii) Phenotypic trait assays

At the end of the long-term experiment, phenotypic trait assays for *Paramecium* from all 16 selection lines were performed under common-garden conditions. Using a micropipette, we arbitrarily picked 4 uninfected paramecia from each selection line and placed them individually in single 1.5 mL Eppendorf tubes filled with bacterised medium, where they were allowed to grow for 2 weeks until small monoclonal lines had established (c. 7-8 asexual generations). Each monoclonal line was then split into three technical replicates and grown for a second common-garden period of 10 days in 50-mL tubes to obtain mass cultures for the phenotype assays (16 selection lines x 4 monoclonal lines x 3 technical replicates = 64 monoclonal lines and 192 replicates, Fig. S3). Of the 64 monoclonal lines, 60 were available to measure 6 phenotypic traits, as follows.

Resistance

To measure resistance, the *Paramecium* were confronted with parasites from core-selection and front-selection lines. We prepared the inocula by mixing the 5 infected core and 5 infected front selection lines, and extracting infectious forms from the two mixes (for details of the extraction protocol, see S2). For

179 inoculation, c. 5000 paramecia were placed in a volume of 25 mL in a 50-mL tube, to which we added 4.5 x
180 10^5 infectious forms (core-parasite or front-parasite inoculum). In this way, we set up 4-8 inoculated tubes
181 per host selection line, balanced between the two parasite inocula (16 selection lines x 2-4 monoclonal lines
182 x 2 technical replicates = 120 inoculated tubes). Four days post-inoculation, we fixed c. 20 individuals from
183 each inoculated replicate with lacto-aceto-orcein [45] and inspected them for absence or presence of
184 infection using a phase-contrast microscope (1000x magnification). We define resistance as the proportion
185 of uninfected individuals in the sample. Preliminary analysis showed that *Paramecium* from the four different
186 selection treatments did not differ in their resistance to the mixes of front or core parasites ($F_{3,12} = 0.44$, n.s.);
187 we therefore combined the two inoculum sources into a single "infected" category for the main analysis.

188 *Dispersal rate*
189 Dispersal was measured in linear 3-patch systems (50 mL tubes; Fig. S4), where the *Paramecium* dispersed
190 from the middle tube into the two outer tubes (see SI for detailed protocol). This system configuration
191 allowed us to use bigger volumes of culture and thus obtain higher numbers of dispersers than in 2-patch
192 systems. Connections were opened for 3 h, dispersal rates were then estimated by counting the *Paramecium*
193 in samples from the central tube (500 µl) and from the combined two outer tubes (3 mL). We employed
194 technical replicates that had not been used for the resistance assay, and were kept in 30 mL of fresh medium
195 for several days prior to the dispersal test. One replicate per monoclonal line was tested (60 dispersal tests).

196 *Population growth rate and equilibrium density*
197 For the population growth assay, we placed groups of 5 arbitrarily picked *Paramecium* in 15-mL tubes filled
198 with 10 mL of bacterised medium. Over 9 days, we tracked densities in 24-h intervals, estimated from the
199 number of individuals present in 200-µL samples. We set up 6-12 tubes per host selection line (3 tubes per
200 monoclonal line), with a total of 180 tubes tested. For each tube, estimates of intrinsic population growth
201 rate (r_0) were obtained by fitting a Beverton-Holt population growth model to each density time series, using
202 a Bayesian approach [52], see section S5 for details). For certain tubes we obtained unsatisfactory fits of
203 equilibrium density; we therefore decided to use the mean density over the second half of the assay (day 5-
204 9) as a proxy for equilibrium density ($\overline{N}$). A small fraction of 19 tubes failed to produce a coherent growth
205 pattern and remained at very low density for unknown reasons; it was not possible to fit our population
206 growth model to these data, and the tubes were therefore excluded from analysis.

207 *Swimming speed and tortuosity*
208 At the end of the above population growth assay, we analysed swimming behaviour, using an established
209 pipeline of computer vision and automated video analysis to collect this data [53,54]. From a given tube, one
210 sample of 119 µL was imaged under a Perfex Pro 10 stereomicroscope, using a Perfex SC38800 camera (15
211 frames per second; duration: 10 s; total magnification: 10x). Videos were analysed using the bemovi R-

package [54], which provided individual-based data on swimming speed and the tortuosity of swimming trajectories (standard deviation of the turning angle distribution). Details of the script video analysis are given in S6. Swimming speed and tortuosity were averaged over all individuals in a sample prior to analysis. A total of 60 samples (1 per monoclonal line) was used for analysis, giving 2-4 observations per host selection line.

Statistical analysis

All statistical analyses were performed with R v 4.1.2 [55]. Focusing on the analysis of trait associations, we constructed a data matrix with the measurements of the 6 traits for 60 monoclonal lines (for resistance, the mean over the two technical replicates was calculated). To impute 10 missing observations in population growth rate and equilibrium density we used the "missMDA" package version 1.16 [56]. Trait distributions were normalised by picking the best transformation ("bestNormalize" package version 1.4.2, [57]). We then performed a multivariate analysis of variance (MANOVA), with range expansion treatment (core vs front selection lines), parasite treatment (infected vs uninfected control selection lines) and their interaction considered as fixed factors. Selection line identity was included as error term. From this same data set, we also performed univariate analyses for each of the 6 traits. In a second step, to better understand the multivariate results, we performed a principal component analysis (PCA), based on the means per selection line and thus a data matrix of 16 x 6 = 96 observations. To complement graphical inspection of results, we used the first and second components (PC1, PC2) for ad-hoc comparisons between treatments. Finally, we conducted correlations among monoclonal lines analysis using a Bayesian approach with the "rstan" package version 2.19.3 [58], details in S7). We considered the three biologically relevant pairs of traits: dispersal-resistance, r_0-$\overline{N}$ and speed-tortuosity.

Results

We found signatures of selection history in the observed phenotypic variation and covariation (Table 1). Univariate analyses showed significant effects of range expansion treatment and/or parasite treatment on all 6 traits (Table 1). Multivariate analysis of the combination of these traits (MANOVA, Table 1) revealed significant effects of the range expansion ($F_{1,12} = 8.69$, $p = 0.005$) and parasite treatment ($F_{1,12} = 8.82$, $p = 0.005$), but not their interaction ($F_{1,12} = 2.68$, $p = 0.111$). Thus, both selection treatments acted jointly, but largely independently, to produce phenotypic differentiation in the *Paramecium*. All examined traits contribute to this divergence, with three pairs of traits forming opposite vectors, pulling treatments in different directions in multi-trait space: dispersal-resistance, r_0-$\overline{N}$ and speed-tortuosity. The presence of parasites changed the intensity and/or sign of the among-line correlation coefficient (Table S1) between these pairs of traits as shown in Figure 2 (full dots vs empty dots).

Table 1 MANOVA and ANOVAs for the effect of range expansion treatment (core vs. front) and parasitism treatment (infected vs. parasite-free populations) on six traits, measured for 16 *P. caudatum* selection lines. P-values < 0.05 highlighted in bold.

		Range expansion		Parasitism		Range x Parasitism
MANOVA	$F_{1, 12}$	p-value	$F_{1, 12}$	p-value	$F_{1, 12}$	p-value
All traits	8.69	**0.005**	8.82	**0.005**	2.68	0.111
ANOVA	$F_{1, 12}$	p-value	$F_{1, 12}$	p-value	$F_{1, 12}$	p-value
Dispersal	1.08	0.318	11.43	**0.005**	1.86	0.197
Resistance	9.91	**0.008**	3.85	0.073	4.44	0.056
Speed	10.03	**0.008**	0.05	0.827	0.14	0.713
Tortuosity	14.82	**0.002**	3.29	0.094	2.29	0.156
r_0	3.72	0.077	0.68	0.425	5.25	**0.040**
$\overline{N}$	2.79	0.120	12.17	**0.004**	4.76	**0.049**

Considering the PCA components, we observed along the horizontal PC1 axis a clear effect of the range expansion treatment (front vs core selection), separating the respective clouds of points (red vs blue Fig. 1). This front / core separation was significant both for the parasite-free selection lines (lower two clouds in Fig. 1, $F_{1,4} = 16.47$, $p = 0.015$), and for selection lines evolving in the presence of the parasite (upper two clouds, $F_{1,4} = 5.83$, $p = 0.042$). The direction and length of the different arrows in Fig. 1 show that these patterns were mainly driven by opposing trends in movement (speed / tortuosity; highest PC 1 loadings, Table S3). Overall, *Paramecium* from the front treatment generally had a lower swimming speed (-12%) and more non-linear movement trajectories (+23% tortuosity) than *Paramecium* from the core treatment (main effects of range expansion treatment: $p < 0.009$; Table 1). The PCA also indicates opposing trends in demography-related traits (Table S3), with lower population growth rate and higher equilibrium density for front selection lines (Fig. 1). However, univariate analyses show that these trends mainly hold for parasite-free control lines (range x parasite interaction: $p < 0.05$; Table 1).

Along the vertical PC2 axis, phenotypic differentiation was mainly determined by the parasite selection treatment (Fig. 1), thus separating selection lines that had been exposed to the parasite and parasite-free lines. The separation was more pronounced for the range front treatment (upper vs lower red clouds, $F_{1,4} = 9.74$, $p = 0.020$) than for the core treatment (upper vs lower blue points, $F_{1,4} = 3.22$, $p = 0.122$). Resistance and dispersal are the key traits associated with the PC2 axis (Table S2), with arrow trajectories indicating higher dispersal for parasite-free lines and higher resistance for lines that had evolved with the parasite (Fig. 1). Univariate analyses confirmed these trends (effects of parasite treatment: $p < 0.07$; Table 1), but also indicate interactions with the range expansion treatment. Thus, the PCA signal for resistance was mainly due

to increased resistance in the front treatment (+ 15%), but not in the core (Fig. 2B; parasite x range treatment: p = 0.056; Table 1). The details of the PCA are provided in Tables S2 and S3. In summary, the experimental treatment combining new front selection conditions with new exposure to parasites produced the strongest phenotypic divergence relative to the negative control treatment (no parasite, no selection for dispersal).

Discussion

Natural populations are currently forced to shift their ranges due to human-induced climatic and environmental changes, which often involves exposure to novel abiotic conditions or confrontation with biotic selection pressures such as parasitism [59,60]. Understanding how ecological dynamics affect the evolution and the trajectory of phenotypic traits in a host-parasite context is of major interest and relevance for conservation, controlling infectious disease and epidemic outbreaks [61,62], as well for the design of proper invasive species management strategies [63]. Importantly, parasites can change the availability of genetic variance to selection as well as the strength and direction of selection. Together with the selective pressures due to range expansion, parasitism will likely produce diverse patterns of divergence and syndromes, leading to changes in the whole host phenotype with trait modifications and the emergence of trade-offs. A multivariate perspective is therefore essential to shed light on how complex traits, like dispersal and resistance, respond to eco-evolutionary pressure in natural populations.

In our study, we find substantial multi-trait divergence between core and front populations of an expanding range. Maximum divergence was observed when both new selection pressures were additively combined (front and parasite treatment). Parasites accentuated the difference between core and front populations for some traits, while reducing it for others. Three pairs of traits, typically involved in differentiation at range fronts, acted as opposing vectors in multi-trait space defining the phenotypic divergence between treatments: dispersal - resistance, r_0 - $\overline{N}$ and swimming speed - tortuosity. In particular, front populations evolved with the parasite were more resistant, but dispersed less than their uninfected counterparts. Even though we may currently not know the precise physiology or morphology underlying these trait relationships, our results illustrate how spatial selection and parasite-mediated selection act jointly to produce major shifts in phenotypic trait space, resulting in multi-facetted dispersal syndromes. Below we focus on the evolutionary forces driving the three trait associations and discuss possible feedbacks of such evolutionary changes on range expansion speed.

Parasitism and dispersal syndromes: effects of the parasite at the front

Dispersal and resistance

In line with theoretical and empirical results on range expansion dynamics, we found evidence for the emergence of dispersal syndromes, with higher levels of dispersal at the range front compared to core populations [23,29,51]. However, the parasite imposed a strong additional selection pressure involving

resistance as key component. Resistance is indeed a major trait selected under parasitism in the *Paramecium* - *Holospora* system [49,64] as well as in many others [65,66], but has so far received relatively little attention in a range expansion context. Here, front populations exposed to the parasite exhibited overall increased resistance, but reduced dispersal, relative to parasite-free populations. Additionally, parasites exacerbated the negative correlation between dispersal and resistance at the front (Figure 2, Table 2), indicating the presence of a trade-off.

Although exceptions are known [67,68], resistance [69] and dispersal [70] are usually considered costly traits, suggesting the potential for a trade-off between the two traits. Thus, the energetic costs of mounting an effective (constitutive) defence against the parasite may reduce the resources available for host dispersal. Similarly, the trade-off may have a behavioural component, linking resistance and feeding activity. Paramecia are filter-feeders and become infected when they ingest infectious spores of the parasite together with other food particles. Hence, resistance may be increased by reducing contact rates with the parasite through reduced feeding activity [71]. Such behavioural aspects of resistance may also include altered swimming behaviour, which could, in turn, affect feeding rates as well as dispersal (see below).

The nature of resistance - dispersal trade-offs may vary from system to system. For example, in bacteria, cell surface modification conferring resistance to bacteriophages might come at the cost of reduced motility [72,73]. Results from selection experiments indicate that the presence of phage can indeed favour bacterial dispersal evolution [72,74]. However, unlike in our study, there was no clear link with resistance, implying that the two traits evolved independently. This suggests that, apart from mechanical or physiological constraints, the emergence of evolutionary trade-offs also depends on the underlying genetic architecture and relationships with fitness, or on the environmental conditions [39,48,75,76].

r_0 and $\overline{N}$

On the demographic axis of the multi-trait space, populations at the range front were characterized by high $\overline{N}$ (equilibrium density) and low r_0 (population growth rate), indicating a trade-off typical of classic r-K selection theory (Fig. 1). This negative correlation was particularly pronounced in the parasite treatment (Fig. 2, Table 2). At first sight, this finding appears in contradiction with common ideas about dispersal syndrome evolution (Burton et al. 2010), predicting competitive strategies in the core (high K or $\overline{N}$) and opportunistic strategies at range fronts (high r_0). However, in our experiment competitive ability is characterised by growth rate, rather than equilibrium density [51,53]. Indeed, the authors showed that rapacious high-growth variants are favoured in the core treatment and more slowly growing variants at the front. This was further corroborated in another study on *P. caudatum*, using both experimental evolution and predictive modelling, again showing the emergence of high $\overline{N}$ and low r_0 at the range front [51]. Comparative evidence suggests

that this may actually be a widespread pattern [77]. Parasite-mediated selection reinforced this pattern and further accentuated the divergence between front and core populations (Fig. 1).

Swimming speed and tortuosity

We found decreased swimming speed for *Paramecium* from the range front treatment, consistent with previous observations [51]. This is opposite to results in a very similar experiment with another ciliate [53] and also seems to contradict observations in other biological systems, where populations at the range front show enhanced movement ability [29,32]. However, in our case, speed reduction was associated with increased swimming tortuosity, i.e., the ability of the individuals to change directions while swimming. This could be considered as an upregulated exploratory behaviour that potentially increases the probability to find the dispersal corridor in our dispersal systems. The negative relationship between these swimming behaviours was accentuated by the presence of the parasite at the range front (Figure 2, Table 2). Thus, similarly to the reinforcement of the above dispersal - resistance and r_0 - $\overline{N}$ relationships, parasite-mediated selection also seems to affect the trait architecture of movement behaviour, i.e., the mechanistic basis of dispersal.

Evo-to-eco feedbacks: Is the evolution with a parasite slowing down range expansions?

The evolution of dispersal syndromes typically produces ecological feedbacks that speed up range expansions [4]. Parasites, in contrast, may keep in check host populations and thereby limit or slow down range fronts, as generically shown for interspecific (antagonistic) interactions [5,9,78]. As discussed above, one of our main results is the emergence of a trade-off between resistance and dispersal. Thus, an intuitive prediction is that, due to lower dispersal, evolution with the parasite slows down the range expansion of infected populations compared to parasite-free populations. This is all the more conceivable given the negative ecological effect of the parasite, via reductions in host density or reduced dispersal [46]. In natural range expansions, instances of resistance evolution against parasites have been described, e.g., at the range front of the cane toad [36]. It is unknown how the resistance evolution in the toad affects dispersal traits, but it seems obvious that, in the face of a detrimental parasite (a lung worm), having the resistance will benefit the range expansion more than not having it.

Beyond these simple considerations, however, answers may be more complex [79], especially when we compare different “strategy sets” (or, dispersal syndromes) in the presence of parasites. Our results suggest that consequences for range expansion speed depend on how the trade-off between dispersal and resistance plays out precisely. If contact rates are high and the parasite virulent, higher levels of resistance may indeed compensate lower dispersal, such that front populations with an evolutionary parasite past might advance faster than their naive, parasite-free counterparts. On the other hand, if enemy-free space can be reached, less resistant variants may actually outrun the parasite and fully profit from their higher dispersal capacity.

These scenarios may, for example, relate to biological invasions, where invaders bring along a parasite to which they have already adapted or, like the cane toad, encounter new parasites at the range front.

For our experimental system, predictions from the present data remain speculative, because relevant measurements (growth, dispersal, movement) were taken in the absence of infection. A full picture would require estimates of virulence/tolerance or dispersal assays that include infected hosts [47,48]. Moreover, future experiments can use multi-microcosm landscapes to actually measure range expansion speeds for the different types of hosts and/or epidemiological scenarios. Ideally, these would be accompanied by theory exploring the simultaneous evolution of dispersal and interaction traits [80] or accounting for additional factors, such as parasite evolution [47], dispersal plasticity [39,48] or the general upregulation of immune responses, known to occur during range expansion [81,82].

Conclusion

Our selection experiment illustrates the possible impact of biotic interactions on evolutionary trajectories during range expansions. Parasite-mediated selection changed the structure of dispersal syndromes, shaping the phenotypic divergence between front and core populations for multiple traits, including dispersal, life-history and resistance. Specifically, increased resistance traded off with a decrease in dispersal, which could potentially slow down range expansion. This study focused on the host, but dispersal syndromes may also evolve in the parasite, or even coevolve. This may further complexify the interplay between spatial selection and biotic (co-)evolution, and make it even more difficult to predict the accompanying ecological feedbacks on range expansion dynamics or disease spread. Replicated range expansions under laboratory conditions represent one tool to disentangle these processes. Although being simplified abstractions of the real world, such experiments may also provide baseline information for applied issues of biocontrol or the monitoring of emerging diseases.

Ethics

Not applicable

Data accessibility

The data from this study are available at https://doi.org/10.5281/zenodo.5907048

Authors' contributions

OK, LN and GZ conceived the study. GZ, LN, MH, EAF, and OK designed the experiments. GZ, LN, CGB and OK performed the experimental work. GZ, LN, OK and EAF performed the statistical analysis. All authors interpreted the results. GZ and OK wrote the first draft of the manuscript and all authors commented on the final version.

Competing interests

The authors declare no competing financial interests.

Funding

This work was funded by the Swiss National Science Foundation (grant no. P2NEP3_184489) to GZ and by the 2019 Godfrey Hewitt Mobility Award granted to LN by ESEB.

Acknowledgements

This is publication ISEM-YYYY-XXX of the Institut des Sciences de l'Evolution - Montpellier.

References

1. Parmesan C, Yohe G. 2003 A globally coherent fingerprint of climate change impacts across natural systems. *Nature* **421**, 37–42. (doi:10.1038/nature01286)

2. Thomas CD *et al.* 2004 Extinction risk from climate change. *Nature* **427**, 145–148. (doi:10.1038/nature02121)

3. Kubisch A, Holt RD, Poethke H-J, Fronhofer EA. 2014 Where am I and why? Synthesizing range biology and the eco-evolutionary dynamics of dispersal. *Oikos* **123**, 5–22. (doi:10.1111/j.1600-0706.2013.00706.x)

4. Miller TEX *et al.* 2020 Eco-evolutionary dynamics of range expansion. *Ecology* **101**, e03139. (doi:10.1002/ecy.3139)

5. Kubisch A, Degen T, Hovestadt T, Poethke HJ. 2013 Predicting range shifts under global change: the balance between local adaptation and dispersal. *Ecography* **36**, 873–882. (doi:10.1111/j.1600-0587.2012.00062.x)

6. Legault G, Bitters ME, Hastings A, Melbourne BA. 2020 Interspecific competition slows range expansion and shapes range boundaries. *Proc. Natl. Acad. Sci.* **117**, 26854–26860. (doi:10.1073/pnas.2009701117)

7. Hochberg ME, Ives AR. 1999 Can natural enemies enforce geographical range limits? *Ecography* **22**, 268–276. (doi:10.1111/j.1600-0587.1999.tb00502.x)

8. Holt RD, Keitt TH. 2000 Alternative causes for range limits: a metapopulation perspective. *Ecol. Lett.* **3**, 41–47. (doi:10.1046/j.1461-0248.2000.00116.x)

9. Price TD, Kirkpatrick M. 2009 Evolutionarily stable range limits set by interspecific competition. *Proc. R. Soc. B Biol. Sci.* **276**, 1429–1434. (doi:10.1098/rspb.2008.1199)

10. Finnerty PB, Shine R, Brown GP. 2018 The costs of parasite infection: Effects of removing lungworms on performance, growth and survival of free-ranging cane toads. *Funct. Ecol.* **32**, 402–415. (doi:10.1111/1365-2435.12992)

11. Kelehear C, Webb JK, Shine R. 2009 Rhabdias pseudosphaerocephala infection in Bufo marinus: lung nematodes reduce viability of metamorph cane toads. *Parasitology* **136**, 919–927. (doi:10.1017/S0031182009006325)

12. Antonovics J, Edwards M. 2011 Spatio-temporal dynamics of bumblebee nest parasites (Bombus subgenus Psythirus ssp.) and their hosts (Bombus spp.). *J. Anim. Ecol.* **80**, 999–1011. (doi:10.1111/j.1365-2656.2011.01846.x)

13. Bradley CA, Altizer S. 2005 Parasites hinder monarch butterfly flight: implications for disease spread in migratory hosts: Parasites and monarch flight. *Ecol. Lett.* **8**, 290–300. (doi:10.1111/j.1461-0248.2005.00722.x)

14. Briers RA. 2003 Range limits and parasite prevalence in a freshwater snail. *Proc. R. Soc. Lond. B Biol. Sci.* **270**, S178–S180. (doi:10.1098/rsbl.2003.0046)

15. Combe M, Gozlan RE. 2018 The rise of the rosette agent in Europe: An epidemiological enigma. *Transbound. Emerg. Dis.* **65**, 1474–1481. (doi:10.1111/tbed.13001)

16. Miller MA, Kinsella JM, Snow RW, Hayes MM, Falk BG, Reed RN, Mazzotti FJ, Guyer C, Romagosa CM. 2018 Parasite spillover: indirect effects of invasive Burmese pythons. *Ecol. Evol.* **8**, 830–840. (doi:10.1002/ece3.3557)

17. Dunn AM *et al.* 2012 Indirect effects of parasites in invasions. *Funct. Ecol.* **26**, 1262–1274. (doi:10.1111/j.1365-2435.2012.02041.x)

18. Strauss A, White A, Boots M. 2012 Invading with biological weapons: the importance of disease-mediated invasions. *Funct. Ecol.* **26**, 1249–1261. (doi:10.1111/1365-2435.12011)

19. Poulin R. 2017 Invasion ecology meets parasitology: Advances and challenges. *Int. J. Parasitol. Parasites Wildl.* **6**, 361–363. (doi:10.1016/j.ijppaw.2017.03.006)

20. Phillips BL, Brown GP, Travis JMJ, Shine R. 2008 Reid's paradox revisited: the evolution of dispersal kernels during range expansion. *Am. Nat.* **172 Suppl 1**, S34-48. (doi:10.1086/588255)

21. Shine R, Brown GP, Phillips BL. 2011 An evolutionary process that assembles phenotypes through space rather than through time. *Proc. Natl. Acad. Sci.* **108**, 5708–5711. (doi:10.1073/pnas.1018989108)

22. Clobert J, Galliard J-FL, Cote J, Meylan S, Massot M. 2009 Informed dispersal, heterogeneity in animal dispersal syndromes and the dynamics of spatially structured populations. *Ecol. Lett.* **12**, 197–209. (doi:10.1111/j.1461-0248.2008.01267.x)

23. Cote J, Bestion E, Jacob S, Travis J, Legrand D, Baguette M. 2017 Evolution of dispersal strategies and dispersal syndromes in fragmented landscapes. *ECOGRAPHY* **40**, 56–73. (doi:10.1111/ecog.02538)

24. Saastamoinen M *et al.* 2018 Genetics of dispersal. *Biol. Rev.* **93**, 574–599. (doi:10.1111/brv.12356)

25. Chuang A, Peterson CR. 2016 Expanding population edges: theories, traits, and trade-offs. *Glob. Change Biol.* **22**, 494–512. (doi:10.1111/gcb.13107)

26. Fjerdingstad EJ, Schtickzelle N, Manhes P, Gutierrez A, Clobert J. 2007 Evolution of dispersal and life history strategies – Tetrahymena ciliates. *BMC Evol. Biol.* **7**, 133. (doi:10.1186/1471-2148-7-133)

27. Brown GP, Phillips BL, Shine R. 2014 The straight and narrow path: the evolution of straight-line dispersal at a cane toad invasion front. *Proc. R. Soc. B Biol. Sci.* **281**, 20141385. (doi:10.1098/rspb.2014.1385)

28. Perkins TA, Phillips BL, Baskett ML, Hastings A. 2013 Evolution of dispersal and life history interact to drive accelerating spread of an invasive species. *Ecol. Lett.* **16**, 1079–1087. (doi:10.1111/ele.12136)

29. Phillips BL, Brown GP, Webb JK, Shine R. 2006 Invasion and the evolution of speed in toads. *Nature* **439**, 803–803. (doi:10.1038/439803a)

30. Lombaert E, Estoup A, Facon B, Joubard B, Grégoire J-C, Jannin A, Blin A, Guillemaud T. 2014 Rapid increase in dispersal during range expansion in the invasive ladybird *Harmonia axyridis*. *J. Evol. Biol.* **27**, 508–517. (doi:10.1111/jeb.12316)

31. Szűcs M, Vahsen ML, Melbourne BA, Hoover C, Weiss-Lehman C, Hufbauer RA. 2017 Rapid adaptive evolution in novel environments acts as an architect of population range expansion. *Proc. Natl. Acad. Sci.* **114**, 13501–13506. (doi:10.1073/pnas.1712934114)

32. Weiss-Lehman C, Hufbauer RA, Melbourne BA. 2017 Rapid trait evolution drives increased speed and variance in experimental range expansions. *Nat. Commun.* **8**, 1–7. (doi:10.1038/ncomms14303)

33. Williams JL, Kendall BE, Levine JM. 2016 Rapid evolution accelerates plant population spread in fragmented experimental landscapes. *Science* **353**, 482–485. (doi:10.1126/science.aaf6268)

34. Lion S, Gandon S. 2015 Evolution of spatially structured host-parasite interactions. *J. Evol. Biol.* **28**, 10–28. (doi:10.1111/jeb.12551)

35. Parratt SR, Numminen E, Laine A-L. 2016 Infectious Disease Dynamics in Heterogeneous Landscapes. *Annu. Rev. Ecol. Evol. Syst.* **47**, 283–306. (doi:10.1146/annurev-ecolsys-121415-032321)

36. Mayer M, Shine R, Brown GP. 2021 Rapid divergence of parasite infectivity and host resistance during a biological invasion. *Biol. J. Linn. Soc.* **132**, 861–871. (doi:10.1093/biolinnean/blaa229)

37. Chaianunporn T, Hovestadt T. 2012 Concurrent evolution of random dispersal and habitat niche width in host-parasitoid systems. *Ecol. Model.* **247**, 241–250. (doi:10.1016/j.ecolmodel.2012.09.005)

38. Chaianunporn T, Hovestadt T. 2012 Evolution of dispersal in metacommunities of interacting species. *J. Evol. Biol.* **25**, 2511–2525. (doi:10.1111/j.1420-9101.2012.02620.x)

39. Deshpande JN, Kaltz O, Fronhofer EA. 2021 Host-parasite dynamics set the ecological theatre for the evolution of state- and context-dependent dispersal in hosts. *OIKOS* **130**, 121–132. (doi:10.1111/oik.07512)

40. Luong LT, Polak M. 2007 Costs of Resistance in the Drosophila–Macrocheles System: A Negative Genetic Correlation Between Ectoparasite Resistance and Reproduction. *Evolution* **61**, 1391–1402. (doi:10.1111/j.1558-5646.2007.00116.x)

41. Sgrò CM, Hoffmann AA. 2004 Genetic correlations, tradeoffs and environmental variation. *Heredity* **93**, 241–248. (doi:10.1038/sj.hdy.6800532)

42. Duffy MA, Forde SE. 2009 Ecological feedbacks and the evolution of resistance. *J. Anim. Ecol.* **78**, 1106–1112. (doi:10.1111/j.1365-2656.2009.01568.x)

43. Kraaijeveld AR, Godfray HCJ. 1997 Trade-off between parasitoid resistance and larval competitive ability in Drosophila melanogaster. *Nature* **389**, 278–280. (doi:10.1038/38483)

44. Wichterman R. 1986 *The Biology of Paramecium*. Springer US. (doi:10.1007/978-1-4757-0372-6)

45. Fokin SI, Görtz H-D. 2009 Diversity of Holospora Bacteria in Paramecium and Their Characterization. In *Endosymbionts in Paramecium* (ed M Fujishima), pp. 161–199. Berlin, Heidelberg: Springer. (doi:10.1007/978-3-540-92677-1_7)

46. Fellous S, Quillery E, Duncan AB, Kaltz O. 2011 Parasitic infection reduces dispersal of ciliate host. *Biol. Lett.* **7**, 327–329. (doi:10.1098/rsbl.2010.0862)

47. Nørgaard LS, Zilio G, Saade C, Gougat-Barbera C, Hall MD, Fronhofer EA, Kaltz O. 2021 An evolutionary trade-off between parasite virulence and dispersal at experimental invasion fronts. *Ecol. Lett.* , ele.13692. (doi:10.1111/ele.13692)

48. Zilio G, Nørgaard LS, Petrucci G, Zeballos N, Gougat-Barbera C, Fronhofer EA, Kaltz O. 2021 Parasitism and host dispersal plasticity in an aquatic model system. *J. Evol. Biol.* , jeb.13893. (doi:10.1111/jeb.13893)

49. Lohse K, Gutierrez A, Kaltz O. 2006 Experimental evolution of resistance in Paramecium caudatum against the bacterial parasite Holospora undulata. *Evolution* **60**, 1177–1186. (doi:10.1111/j.0014-3820.2006.tb01196.x)

50. Duncan AB, Fellous S, Kaltz O. 2011 Temporal variation in temperature determines disease spread and maintenance in Paramecium microcosm populations. *Proc. R. Soc. B Biol. Sci.* **278**, 3412–3420. (doi:10.1098/rspb.2011.0287)

51. Zilio G, Krenek S, Gougat-Barbera C, Fronhofer EA, Kaltz O. 2022 Predicting evolution in experimental range expansions of an aquatic model system. , 2022.01.20.477128. (doi:10.1101/2022.01.20.477128)

52. Rosenbaum B, Raatz M, Weithoff G, Fussmann GF, Gaedke U. 2019 Estimating Parameters From Multiple Time Series of Population Dynamics Using Bayesian Inference. *Front. Ecol. Evol.* **6**. (doi:10.3389/fevo.2018.00234)

53. Fronhofer EA, Altermatt F. 2015 Eco-evolutionary feedbacks during experimental range expansions. *Nat. Commun.* **6**, 6844. (doi:10.1038/ncomms7844)

54. Pennekamp F, Schtickzelle N, Petchey OL. 2015 BEMOVI, software for extracting behavior and morphology from videos, illustrated with analyses of microbes. *Ecol. Evol.* **5**, 2584–2595. (doi:10.1002/ece3.1529)

55. R Core Team. In press. R: A language and environment for statistical computing. *R Found. Stat. Comput. Vienna Austria URL HttpswwwR-Proj.*

56. Josse J, Husson F. 2016 missMDA: A Package for Handling Missing Values in Multivariate Data Analysis. *J. Stat. Softw.* **70**, 1–31. (doi:10.18637/jss.v070.i01)

533 57. Peterson RA, Cavanaugh JE. 2019 Ordered quantile normalization: a semiparametric transformation
534 built for the cross-validation era. *J. Appl. Stat.* **0**, 1–16. (doi:10.1080/02664763.2019.1630372)

535 58. Carpenter B *et al.* 2017 Stan: A Probabilistic Programming Language. *J. Stat. Softw.* **76**, 1–32.
536 (doi:10.18637/jss.v076.i01)

537 59. Bowler DE *et al.* 2020 Mapping human pressures on biodiversity across the planet uncovers
538 anthropogenic threat complexes. *People Nat.* **2**, 380–394. (doi:10.1002/pan3.10071)

539 60. Morales-Castilla I, Pappalardo P, Farrell MJ, Aguirre AA, Huang S, Gehman A-LM, Dallas T, Gravel D,
540 Davies TJ. 2021 Forecasting parasite sharing under climate change. *Philos. Trans. R. Soc. B Biol. Sci.* **376**,
541 20200360. (doi:10.1098/rstb.2020.0360)

542 61. Halloran ME, Longini IM. 2014 Emerging, evolving, and established infectious diseases and
543 interventions. *Science* **345**, 1292–1294. (doi:10.1126/science.1254166)

544 62. Smith KF, Goldberg M, Rosenthal S, Carlson L, Chen J, Chen C, Ramachandran S. 2014 Global rise in
545 human infectious disease outbreaks. *J. R. Soc. Interface* **11**, 20140950. (doi:10.1098/rsif.2014.0950)

546 63. Crowley SL, Hinchliffe S, McDonald RA. 2017 Conflict in invasive species management. *Front. Ecol.*
547 *Environ.* **15**, 133–141. (doi:10.1002/fee.1471)

548 64. Duncan AB, Fellous S, Kaltz O. 2011 Reverse Evolution: Selection Against Costly Resistance in Disease-
549 Free Microcosm Populations of Paramecium Caudatum. *Evolution* **65**, 3462–3474. (doi:10.1111/j.1558-
550 5646.2011.01388.x)

551 65. Brockhurst MA, Buckling A, Poullain V, Hochberg ME. 2007 The impact of migration from parasite-free
552 patches on antagonistic host-parasite coevolution. *EVOLUTION* **61**, 1238–1243. (doi:10.1111/j.1558-
553 5646.2007.00087.x)

554 66. Lennon JT, Khatana SAM, Marston MF, Martiny JBH. 2007 Is there a cost of virus resistance in marine
555 cyanobacteria? *ISME J.* **1**, 300–312. (doi:10.1038/ismej.2007.37)

556 67. Auld SKJR, Penczykowski RM, Ochs JH, Grippi DC, Hall SR, Duffy MA. 2013 Variation in costs of parasite
557 resistance among natural host populations. *J. Evol. Biol.* **26**, 2479–2486. (doi:10.1111/jeb.12243)

558 68. Labbé P, Vale PF, Little TJ. 2010 Successfully resisting a pathogen is rarely costly in Daphnia magna.
559 *BMC Evol. Biol.* **10**, 355. (doi:10.1186/1471-2148-10-355)

69. Schmid-Hempel P. 2003 Variation in immune defence as a question of evolutionary ecology. *Proc. R. Soc. B Biol. Sci.* **270**, 357–366. (doi:10.1098/rspb.2002.2265)

70. Bonte D *et al.* 2012 Costs of dispersal. *Biol. Rev.* **87**, 290–312. (doi:10.1111/j.1469-185X.2011.00201.x)

71. Fels D, Vignon M, Kaltz O. 2008 Ecological and genetic determinants of multiple infection and aggregation in a microbial host-parasite system. *Parasitology* **135**, 1373–1383. (doi:10.1017/S0031182008004940)

72. Koskella B, Taylor TB, Bates J, Buckling A. 2011 Using experimental evolution to explore natural patterns between bacterial motility and resistance to bacteriophages. *ISME J.* **5**, 1809–1817. (doi:10.1038/ismej.2011.47)

73. Whitchurch CB, Mattick JS. 1994 Escherichia coli contains a set of genes homologous to those involved in protein secretion, DNA uptake and the assembly of type-4 fimbriae in other bacteria. *Gene* **150**, 9–15. (doi:10.1016/0378-1119(94)90851-6)

74. Taylor TB, Buckling A. 2013 Bacterial motility confers fitness advantage in the presence of phages. *J. Evol. Biol.* **26**, 2154–2160. (doi:10.1111/jeb.12214)

75. Boots M. 2011 The Evolution of Resistance to a Parasite Is Determined by Resources. *Am. Nat.* **178**, 214–220. (doi:10.1086/660833)

76. Meaden S, Paszkiewicz K, Koskella B. 2015 The cost of phage resistance in a plant pathogenic bacterium is context-dependent. *Evol. Int. J. Org. Evol.* **69**, 1321–1328. (doi:10.1111/evo.12652)

77. Dallas T, Park AW, Drake JM. 2017 Predicting cryptic links in host-parasite networks. *PLOS Comput. Biol.* **13**. (doi:10.1371/journal.pcbi.1005557)

78. Moorcroft PR, Pacala SW, Lewis MA. 2006 Potential role of natural enemies during tree range expansions following climate change. *J. Theor. Biol.* **241**, 601–616. (doi:10.1016/j.jtbi.2005.12.019)

79. Barnett LK, Phillips BL, Heath ACG, Coates A, Hoskin CJ. 2018 The impact of parasites during range expansion of an invasive gecko. *Parasitology* **145**, 1400–1409. (doi:10.1017/S003118201800015X)

80. Drown DM, Dybdahl MF, Gomulkiewicz R. 2013 Consumer–Resource Interactions and the Evolution of Migration. *Evolution* **67**, 3290–3304. (doi:10.1111/evo.12194)

81. Diagne C *et al.* 2017 Contemporary variations of immune responsiveness during range expansion of two invasive rodents in Senegal. *Oikos* **126**, 435–446. (doi:10.1111/oik.03470)

588 82. Gardner ST, Assis VR, Smith KM, Appel AG, Mendonça MT. 2020 Innate immunity of Florida cane toads:
589 how dispersal has affected physiological responses to LPS. *J. Comp. Physiol. [B]* **190**, 317–327.
590 (doi:10.1007/s00360-020-01272-7)

591

592 Figure captions

593 **Figure 1** PCA for six traits measured for 16 long-term selection lines of *P. caudatum*, showing the first two
594 principal component axes, PC1 and PC2. The length of the thin arrows inside the graph represents the loading
595 values; the longer the arrow the higher the correlation with the PC axis and the variance explained by that
596 trait. Each point represents the average phenotypic value of a given selection line in multivariate space, with
597 long-term treatment origins specified: range core (blue) vs. range front (red) treatment; evolved in the
598 presence (full circles) vs. absence (empty circles) of the parasite *H. undulata*. The blue empty circles with
599 dotted ellipsis represent the ancestral host populations. The ellipses represent the containment probability
600 region of the multivariate space for the four treatments.

601 **Figure 2** Trait correlations for *P. caudatum* evolved in range core and range front treatments: (A-B) dispersal
602 - resistance, (C-D) growth rate (r_0) - equilibrium density ($\overline{N}$) and (E-F) swimming speed - swimming tortuosity.
603 For each panel, the parasitism treatment is specified: evolved in the presence of the parasite (full dots and
604 lines) vs. parasite-free (dashed dots and lines). The points are the means for 60 monoclonal cultures, isolated
605 from a total of 16 long-term selection lines (for details, see text). Correlations were obtained with Bayesian
606 inference, separately for each combination of range expansion and parasitism treatments. Ellipses are bound
607 to non-linear space and represent the 10, 25, 50, 75 an 90 % CI of the correlation of pairs of traits.
608 Distributions in the small panels represent the posterior distributions of the correlation coefficients, the
609 dashed black line highlight the 0 value, and thus the absence of correlation.

610

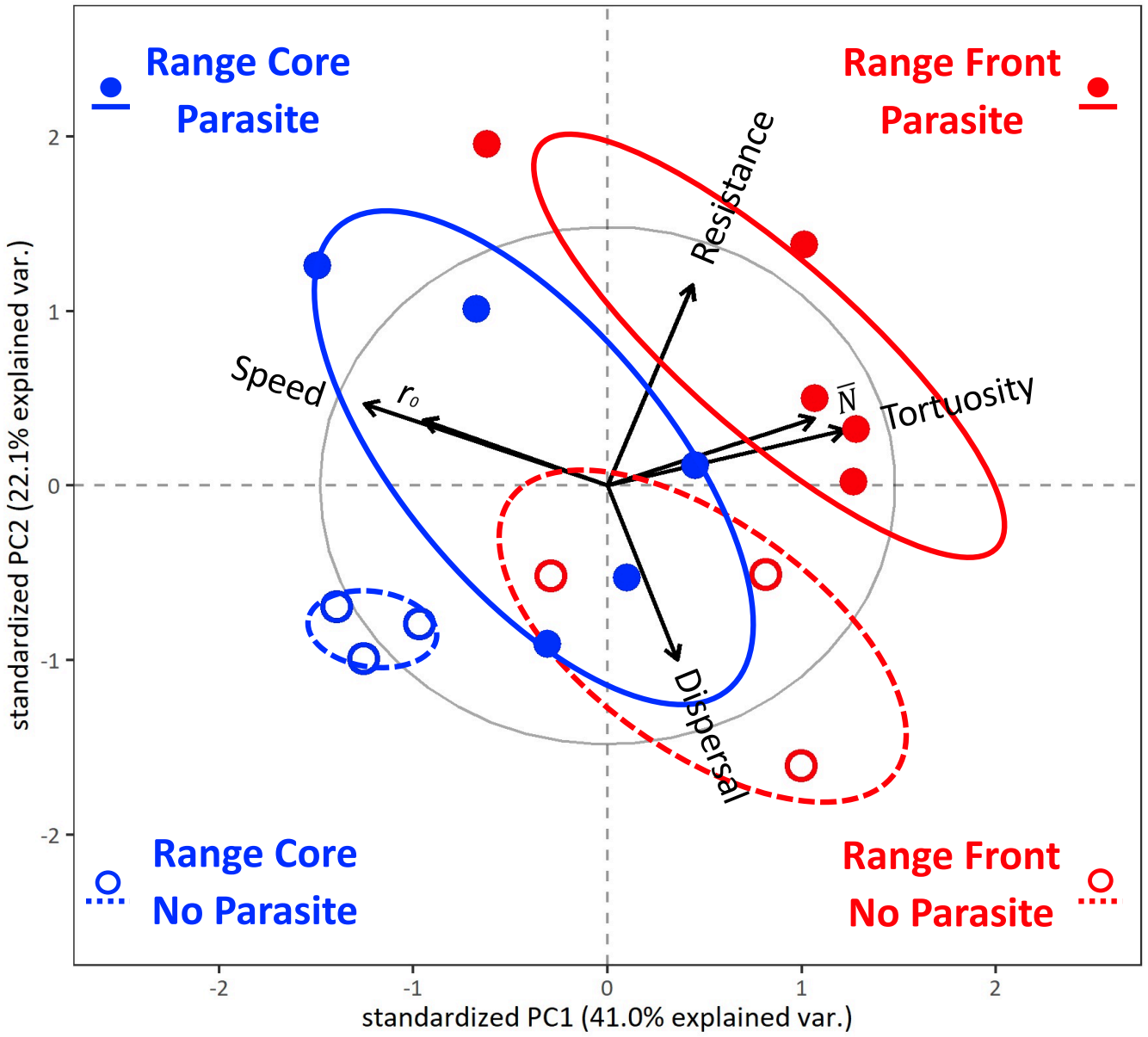
Range Core
Parasite
Range Front
Parasite
Range Core
No Parasite
Range Front
No Parasite
Resistance
Speed
r_o
$\overline{N}$
Tortuosity
Dispersal
standardized PC2 (22.1% explained var.)
standardized PC1 (41.0% explained var.)
2
1
0
-1
-2
-2
-1
0
1
2